

Towards a data-driven analysis of hadronic light-by-light scattering

Gilberto Colangelo^a, Martin Hoferichter^a, Bastian Kubis^b, Massimiliano Procura^a, Peter Stoffer^a

^aAlbert Einstein Center for Fundamental Physics, Institute for Theoretical Physics, Universität Bern, Sidlerstrasse 5, CH-3012 Bern, Switzerland

^bHelmholtz-Institut für Strahlen- und Kernphysik (Theorie) and Bethe Center for Theoretical Physics, Universität Bonn, D-53115 Bonn, Germany

Abstract

The hadronic light-by-light contribution to the anomalous magnetic moment of the muon was recently analyzed in the framework of dispersion theory, providing a systematic formalism where all input quantities are expressed in terms of on-shell form factors and scattering amplitudes that are in principle accessible in experiment. We briefly review the main ideas behind this framework and discuss the various experimental ingredients needed for the evaluation of one- and two-pion intermediate states. In particular, we identify processes that in the absence of data for doubly-virtual pion–photon interactions can help constrain parameters in the dispersive reconstruction of the relevant input quantities, the pion transition form factor and the helicity partial waves for $\gamma^*\gamma^* \rightarrow \pi\pi$.

Keywords: Dispersion relations, anomalous magnetic moment of the muon, Compton scattering, meson–meson interactions

PACS: 11.55.Fv, 13.40.Em, 13.60.Fz, 13.75.Lb

1. Introduction

The limiting factor in the accuracy of the Standard-Model prediction for the anomalous magnetic moment of the muon $a_\mu = (g-2)_\mu/2$ is control over hadronic uncertainties [1, 2]. The leading hadronic contribution, hadronic vacuum polarization, is related to the total hadronic cross section in e^+e^- annihilation, so that the improvements necessary to compete with the projected accuracy of the FNAL and J-PARC experiments can be achieved with a dedicated e^+e^- program, see e.g. [3, 4]. Owing to the complexity of the hadronic light-by-light (HLbL) tensor, a similar data-driven approach for the subleading¹ HLbL scattering contribution has only recently been suggested, and only for the leading hadronic channels [8]. In contrast to previous approaches [9–21], this formalism aims at providing a direct link between data and the HLbL contribution to a_μ . An alternative strategy to reduce model-dependence in HLbL relies on lattice QCD, see [22] for a first calculation.

The dispersive framework in [8] includes both the dominant pseudoscalar-pole contributions as well as two-meson intermediate states, thus covering the most important channels. In view of the fact that a data-driven approach for the HLbL contribution is substantially more involved than that for HVP, we present here an overview of this approach leaving aside all theoretical details, and emphasize which measurements can help constrain the required hadronic input. At present such an overview can only be obtained after studying several different theoretical papers. It is, however, essential that also experimentalists become fully aware that some measurements may have a substantial and model-independent impact on a better determi-

nation of the HLbL contribution to a_μ . This is the main aim of the present letter.

2. Theoretical framework

2.1. Dispersion relations

In dispersion theory the matrix element of interest is reconstructed from information on its analytic structure: residues of poles, discontinuities along cuts, and subtraction constants (representing singularities at infinity). In contrast to HVP, the complexity of the HLbL tensor prohibits the summation of all possible intermediate states into a single dispersion relation. Instead, one has to rely on an expansion in the mass of allowed intermediate states, justified by higher thresholds and phase-space suppression in the dispersive integrals. In this paper we concentrate on the lowest-lying intermediate states, the π^0 pole and $\pi\pi$ cuts, that illustrate the basic features of our dispersive approach and are expected to be most relevant numerically. We will comment on higher intermediate states in Sect. 4.

Given that each contribution to the HLbL tensor is uniquely defined by its analytic structure, it can be related unambiguously to a certain physical intermediate state. We decompose the HLbL tensor according to

$$\Pi_{\mu\nu\lambda\sigma} = \Pi_{\mu\nu\lambda\sigma}^{\pi^0} + \Pi_{\mu\nu\lambda\sigma}^{\text{FsQED}} + \Pi_{\mu\nu\lambda\sigma}^{\pi\pi} + \dots, \quad (1)$$

where $\Pi_{\mu\nu\lambda\sigma}^{\pi^0}$ denotes the pion pole, $\Pi_{\mu\nu\lambda\sigma}^{\text{FsQED}}$ the amplitude in scalar QED with vertices dressed by the pion vector form factor F_π^V (FsQED), $\Pi_{\mu\nu\lambda\sigma}^{\pi\pi}$ includes the remaining $\pi\pi$ contribution, and the ellipsis higher intermediate states. Representative unitarity diagrams for each term are shown in Fig. 1.

The separation of the FsQED amplitude ensures that contributions with simultaneous cuts in two kinematic variables are correctly accounted for. In fact, $\Pi_{\mu\nu\lambda\sigma}^{\text{FsQED}}$ is completely fixed by

¹At this order also two-loop diagrams with insertions of hadronic vacuum polarization appear [5]. Even higher-order hadronic contributions have been recently considered in [6, 7].

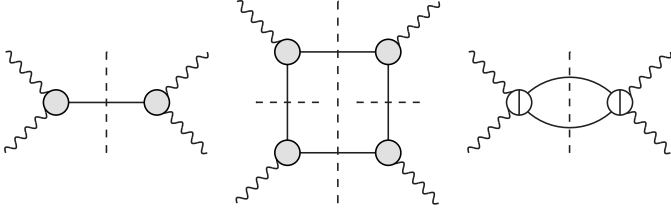


Figure 1: Representative unitarity diagrams for the pion pole (left), the FsQED contribution (middle), and $\pi\pi$ rescattering (right). The gray blobs refer to the pertinent pion form factors, those with vertical line to the non-pole $\gamma^*\gamma^* \rightarrow \pi\pi$ amplitude. The dashed lines indicate the cutting of pion propagators. For more details see [8].

the pion vector form factor, see [8] for details and explicit expressions. Since for this purpose F_π^V is known to sufficient accuracy experimentally, $\Pi_{\mu\nu\lambda\sigma}^{\text{FsQED}}$ is completely determined and we will concentrate on reviewing the central results for $\Pi_{\mu\nu\lambda\sigma}^{\pi^0}$ and $\Pi_{\mu\nu\lambda\sigma}^{\pi\pi}$ in the following.

2.2. Pion pole

The residue of the pion pole is determined by the pion transition form factor $\mathcal{F}_{\pi^0\gamma^*\gamma^*}(q_1^2, q_2^2)$. The corresponding contribution to a_μ follows from [17]

$$\begin{aligned} a_\mu^{\pi^0} &= -e^6 \int \frac{d^4 q_1}{(2\pi)^4} \int \frac{d^4 q_2}{(2\pi)^4} \frac{1}{q_1^2 q_2^2 s Z_1 Z_2} \\ &\times \left\{ \frac{\mathcal{F}_{\pi^0\gamma^*\gamma^*}(q_1^2, q_2^2) \mathcal{F}_{\pi^0\gamma^*\gamma^*}(s, 0)}{s - M_{\pi^0}^2} T_1^{\pi^0}(q_1, q_2; p) \right. \\ &\quad \left. + \frac{\mathcal{F}_{\pi^0\gamma^*\gamma^*}(s, q_1^2) \mathcal{F}_{\pi^0\gamma^*\gamma^*}(q_1^2, 0)}{q_1^2 - M_{\pi^0}^2} T_2^{\pi^0}(q_1, q_2; p) \right\}, \\ Z_1 &= (p + q_1)^2 - m^2, \quad Z_2 = (p - q_2)^2 - m^2, \\ s &= (q_1 + q_2)^2, \end{aligned} \quad (2)$$

where m denotes the mass of the muon, p its momentum, $e = \sqrt{4\pi\alpha}$ the electric charge, and the $T_i^{\pi^0}(q_1, q_2; p)$ are known kinematic functions.

It should be mentioned that the relation (2) only represents the π^0 pole, it does not, on its own, satisfy QCD short-distance constraints. As pointed out in [19], the pion pole as defined in (2) tends faster to zero for large q^2 than required by perturbative QCD due to the momentum dependence in the singly-virtual form factors. The correct high-energy behavior is only restored by the exchange of heavier pseudoscalar resonances, but the pion-pole contribution, by its strict dispersive definition, is unambiguously given as stated in (2).

2.3. $\pi\pi$ intermediate states

The contribution from $\pi\pi$ intermediate states can be expressed as [8]

$$a_\mu^{\pi\pi} = e^6 \int \frac{d^4 q_1}{(2\pi)^4} \int \frac{d^4 q_2}{(2\pi)^4} \frac{\sum_i I_i(s, q_1^2, q_2^2) T_i^{\pi\pi}(q_1, q_2; p)}{q_1^2 q_2^2 s Z_1 Z_2}, \quad (3)$$

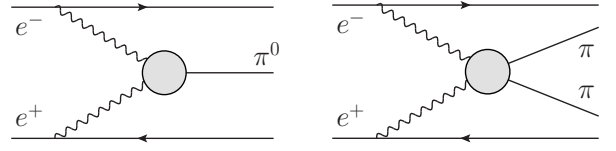


Figure 2: $e^+e^- \rightarrow e^+e^-\pi^0$ and $e^+e^- \rightarrow e^+e^-\pi\pi$ in space-like kinematics.

in a way similar to the pion pole (2). The $T_i^{\pi\pi}(q_1, q_2; p)$ again denote known kinematic functions, while the information on the amplitude on the cut is hidden in the dispersive integrals $I_i(s, q_1^2, q_2^2)$. For instance, the first S -wave term reads

$$\begin{aligned} I_1(s, q_1^2, q_2^2) &= \frac{1}{\pi} \int_{4M_\pi^2}^{\infty} \frac{ds'}{s' - s} \left[\left(\frac{1}{s' - s} - \frac{s' - q_1^2 - q_2^2}{\lambda(s', q_1^2, q_2^2)} \right) \right. \\ &\quad \times \text{Im} h_{++++}^0(s'; q_1^2, q_2^2; s, 0) \\ &\quad \left. + \frac{2\xi_1\xi_2}{\lambda(s', q_1^2, q_2^2)} \text{Im} h_{00,++}^0(s'; q_1^2, q_2^2; s, 0) \right] \end{aligned} \quad (4)$$

with Källén function $\lambda(x, y, z) = x^2 + y^2 + z^2 - 2(xy + xz + yz)$, normalization of longitudinal polarization vectors ξ_i , and partial-wave helicity amplitudes $h_{\lambda_1\lambda_2\lambda_3\lambda_4}^J(s; q_1^2, q_2^2; q_3^2, q_4^2)$ for

$$\gamma^*(q_1, \lambda_1) \gamma^*(q_2, \lambda_2) \rightarrow \gamma^*(q_3, \lambda_3) \gamma^*(q_4, \lambda_4) \quad (5)$$

with angular momentum J . By means of partial-wave unitarity

$$\begin{aligned} \text{Im} h_{\lambda_1\lambda_2\lambda_3\lambda_4}^J(s; q_1^2, q_2^2; q_3^2, q_4^2) \\ = \frac{\sqrt{1 - 4M_\pi^2/s}}{16\pi} h_{J,\lambda_1\lambda_2}(s; q_1^2, q_2^2) h_{J,\lambda_3\lambda_4}(s; q_3^2, q_4^2), \end{aligned} \quad (6)$$

the imaginary part in (4) is related to the helicity partial waves $h_{J,\lambda_1\lambda_2}(s; q_1^2, q_2^2)$ for $\gamma^*\gamma^* \rightarrow \pi\pi$, which have to be determined from experiment.

One key feature in the derivation of (3) concerns the subtraction polynomial. Frequently, dispersion relations need to be subtracted to render the integrals convergent, and the ensuing subtraction constants are free parameters of the approach that need to be determined either from experiment or by further theoretical means, such as effective field theories or lattice QCD. For HLbL scattering, however, gauge invariance puts very stringent constraints on the amplitude and the subtraction polynomial. Therefore, the situation is actually similar to HVP, where the combination of analyticity, unitarity, and gauge invariance provides a parameter-free relation between the contribution to a_μ and the experimental input, the hadronic e^+e^- cross section, as well.

3. Experimental input

By means of a Wick rotation the loop integrals in (2) and (3) can be brought into such a form that only space-like momenta appear in the integral, so that in principle all required information can be extracted from the processes depicted in Fig. 2.

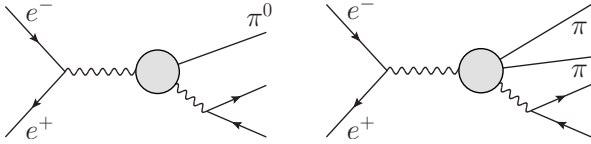


Figure 3: $e^+e^- \rightarrow e^+e^-\pi^0$ and $e^+e^- \rightarrow e^+e^-\pi\pi$ in time-like kinematics.

However, this would require double-tag measurements for arbitrary negative virtualities, and, in the $\pi\pi$ case, sufficient angular information to perform a partial-wave analysis.

Although such detailed information about doubly-virtual pion-photon interactions is currently not available, there are existing and planned measurements involving real or singly-virtual processes, not only in space-like but also in time-like kinematics, see Fig. 3 for the doubly-virtual time-like case. All this information can be used to reconstruct, in turn, both the pion transition form factor as well as $\gamma^*\gamma^* \rightarrow \pi\pi$ partial waves using dispersion relations. The benefits from such a program are manifold: first, it makes sure that the resulting input for (2) and (3) is consistent with analyticity and unitarity. Second, it would allow for a global analysis of all information of pion-photon interactions from all kinematic regions. Third, it should allow for the identification of processes and kinematic regions that are responsible for the largest uncertainty in the final HLbL prediction and should therefore be subject to further experimental scrutiny. In this paper we do not yet make quantitative statements, but rather identify processes potentially relevant, as well as overlap in the calculation of the one- and two-pion input.

For the pion transition form factor some work along these lines has already been presented in [23–27]. Similarly, analyses of the on-shell process $\gamma\gamma \rightarrow \pi\pi$ [28, 29], the singly-virtual reaction $\gamma^*\gamma \rightarrow \pi\pi$ [30], and, some first steps, for the doubly-virtual case $\gamma^*\gamma^* \rightarrow \pi\pi$ [31] have been performed. In particular, in [31] it was shown how to properly account for so-called anomalous thresholds [32, 33], which emerge in time-like kinematics for $\gamma^*\gamma^* \rightarrow \pi\pi$ as a new feature concerning the analytic properties of the scattering amplitude.

A collection of processes relevant for the execution of this program for one- and two-pion intermediate states is shown in Fig. 4. The line coding is such that gray boxes refer to the final ingredients for a_μ , black ones to quantities considered as input, and dashed boxes to quantities that can both be measured and calculated theoretically. The last class of processes serves as a check of agreement between experiment and theory at various stages: the theoretical representations are often confined to *elastic* unitarity and include at most $\pi\pi$ intermediate states, while some quantities, such as the pion vector form factor F_V^π , are known experimentally to much higher precision, and at higher energies than accessible to the elastic approximation. In this way, the difference between the full experimental result and the dispersive reconstruction can be taken as indicative of the impact of higher intermediate states.

3.1. Pion transition form factor

One of the central building blocks in Fig. 4 is $\pi\pi$ scattering, whose phase shifts, by virtue of Watson’s final-state theorem [34], are required for the resummation of $\pi\pi$ rescattering corrections. The corresponding analyses of $\omega, \phi \rightarrow 3\pi$ [24] and $\gamma\pi \rightarrow \pi\pi$ [25] give then access to the pion transition form factor with the isoscalar virtuality either fixed to the mass of ω, ϕ or to a real isoscalar photon, respectively. In particular, the formalism provides a parametrization of $\gamma\pi \rightarrow \pi\pi$ that can be used to extract the chiral $\gamma 3\pi$ anomaly from data and thereby check the underlying low-energy theorem. For general isoscalar virtualities the normalization of the amplitude cannot be predicted within dispersion theory, but has to be fitted to data for the $e^+e^- \rightarrow 3\pi$ spectrum. Combining the isoscalar and isovector channels allows for the confrontation with $e^+e^- \rightarrow \pi^0\gamma$ data [35].

In order to illustrate the predictive power of the dispersive representation of the various amplitudes, we discuss the number of subtractions in the program outlined above in some more detail. Both $\omega, \phi \rightarrow 3\pi$ and $\gamma\pi \rightarrow \pi\pi$ are dominated by a single partial wave (the P -wave), and standard arguments on a realistic high-energy behavior suggest a single subtraction constant should in principle be sufficient. This is given by the chiral anomaly $F_{3\pi}$ for $\gamma\pi \rightarrow \pi\pi$ (and can be used as theoretical input in the absence of a precise experimental extraction [25]), and can be determined from the partial decay widths $\Gamma_{3\pi}$ of $\omega, \phi \rightarrow 3\pi$ for the decays [24]. Such singly-subtracted three-pion partial waves subsequently allow for an unsubtracted dispersion relation for the corresponding transition form factors (with the charged-pion vector form factor as its sole additional input); in particular, sum rules exist for the decay widths $\Gamma_{\pi^0\gamma}$ of $\omega, \phi \rightarrow \pi^0\gamma$ [26] as well as for the chiral anomaly $F_{\pi^0\gamma\gamma}$ for $\pi^0 \rightarrow \gamma\gamma$ [25]. A representation of the corresponding unitarity relations, together with the list of necessary and optional subtractions, is given in Table 1. The first panel refers to the process with vanishing isoscalar virtuality $q_s^2 = 0$, the second to $q_s^2 = M_\omega^2, M_\phi^2$, and the third to the general case.

As all these dispersion relations are constrained to *elastic* unitarity, i.e. only take two-pion intermediate states (in the isovector P -wave channel) into account, the accuracy of these is expected not to be perfect, and indeed can be checked experimentally. A high-statistics Dalitz plot for $\phi \rightarrow 3\pi$ [36] was shown to be described perfectly only as soon as a second subtraction was introduced to improve the convergence of the dispersive integrals, and to suppress inelastic effects [24]. Similarly, the theoretical amplitude to accurately extract the $\gamma 3\pi$ anomaly from data was also formulated as a two-parameter, twice-subtracted representation for the cross section $\sigma(\gamma\pi \rightarrow \pi\pi)$ [25]. The above-mentioned sum rules for transition form factor normalizations are found to be saturated by two-pion intermediate states at the 90% level; very similar results were also found for the (singly-virtual) η transition form factor [37]. In the general case, a second subtraction could be implemented by interpolating between $q_s^2 = 0$ and $q_s^2 = M_\omega^2, M_\phi^2$ with a representation analogous to the one used for the $e^+e^- \rightarrow 3\pi$ spectrum [35].

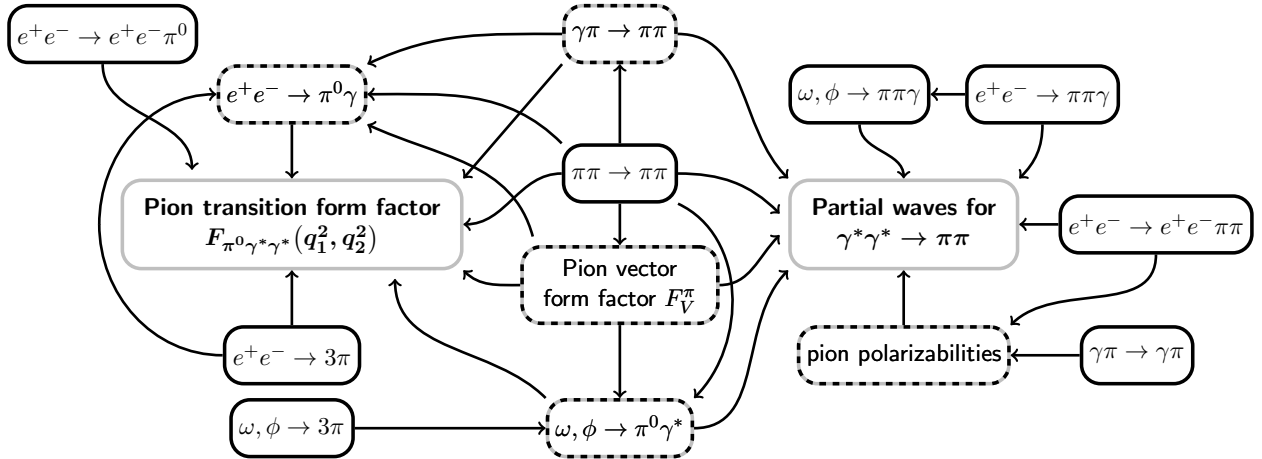


Figure 4: Processes relevant for the dispersive reconstruction of the pion transition form factor and the helicity partial waves for $\gamma^*\gamma^* \rightarrow \pi\pi$.

While improving on the accuracy of dispersive representations at low energies, additional subtractions in general lead to less convergent amplitudes in the high-energy limit. In this sense, the number of subtractions chosen for the $\gamma^* \rightarrow 3\pi$ partial waves cannot be considered independently of the dispersive representation for the transition form factors constructed therewith: in principle, oversubtracted partial waves for $e^+e^- \rightarrow 3\pi$ also necessitate a further subtraction for the transition form factors. For example, for a twice-subtracted $\omega \rightarrow 3\pi$ partial wave, there is no formally convergent sum rule for the amplitude $\omega \rightarrow \pi^0\gamma$ (although the contribution to the dispersive integral from the low-energy region below 1 GeV may in practice differ very little). In this sense, the two columns for indispensable (SC 1) and optional (SC 2) subtractions in Table 1 are required to be applied consistently (with the exception of the last line concerning the parametrization of the $e^+e^- \rightarrow 3\pi$ cross section, which concerns a different kinematical variable, the three-pion invariant mass).

We expect to improve on the convergence of the dispersive calculation of the q^2 -dependence of the transition form factors when oversubtracting them once. In this way, the singly-virtual π^0 transition form factor as tested in $e^+e^- \rightarrow \pi^0\gamma$, in the last step, serves as input to fix a subtraction function required for a reliable prediction of the full doubly-virtual transition form factor. Complementary information extracted from $e^+e^- \rightarrow e^+e^-\pi^0$ directly, either in the time-like or space-like region, provides further checks of consistency and could potentially improve the accuracy of the form-factor determination.

3.2. Partial waves for $\gamma^*\gamma^* \rightarrow \pi\pi$

Several of the quantities mentioned in the context of the pion transition form factor also feature prominently in the calculation of the helicity partial waves for $\gamma^*\gamma^* \rightarrow \pi\pi$. First of all, $\pi\pi$ scattering determines their unitarity relation, i.e. their right-hand cut. The leading contribution to the left-hand cut is generated by the pion pole, with the coupling to the virtual photons described by the pion vector form factor. Multi-pion contributions to the left-hand cut are usually approximated in an effec-

tive resonance description, e.g. 2π would correspond to the ρ and 3π to ω, ϕ (and, at higher energies, to the axial-vector a_1). The widths of ω, ϕ are sufficiently small that a narrow-width approximation is justified, so that the coupling to the virtual photons is governed by the ω, ϕ transition form factors. In contrast, the width of the ρ can be strictly incorporated by expressing its contribution in terms of a dispersive integral with spectral function determined by the P -wave for $\gamma^*\pi \rightarrow \pi\pi$, one of the processes already appearing in the context of the pion transition form factor. A representation of these building blocks for the description of the left-hand cut is given in the upper panel of Table 2.²

An important aspect of the dispersive reconstruction of $\gamma^*\gamma^* \rightarrow \pi\pi$ concerns subtraction functions [28–30], at least one subtraction appears to be necessary in most partial waves. In the on-shell case, the subtraction constants may be identified with pion polarizabilities and either taken from experiment or from Chiral Perturbation Theory (ChPT): one subtraction requires knowledge of the dipole polarizabilities $\alpha_1 \pm \beta_1$, while a second subtraction involves also the quadrupole polarizabilities $\alpha_2 \pm \beta_2$. In general, however, the subtraction constants become functions of the virtualities of the photons. As long as these virtualities are small, the prediction from ChPT is available, but beyond the range of validity of the chiral expansion data input is needed. In [30] data for $e^+e^- \rightarrow \pi\pi\gamma$ were used to fix the subtraction function for the singly-virtual case. Again, the strength of the dispersive approach is that this information collected in the time-like region can be carried over to space-like kinematics, even though for the doubly-virtual case control over anomalous thresholds is crucial [31]. All data on $e^+e^- \rightarrow e^+e^-\pi\pi$, be it in the real, singly-, or doubly-virtual case, would help constrain the subtraction functions, for which, in turn, one may analyze a dispersive representation, with subtraction constants fixed by ChPT and discontinuities by data on $e^+e^- \rightarrow \pi\pi\gamma$ and

²In this discussion, we confine ourselves to (multi-)pion intermediate states only. With the (isoscalar) photon virtuality at the ϕ mass, the left-hand cut will be dominated by kaon pole terms, rather than by two pions; see Sect. 4 for the $\pi\pi/K\bar{K}$ coupled-channel system.

process	unitarity relations	SC 1	SC 2
	 	$F_{3\pi}$	$F_{\pi^0\gamma\gamma}$ $\sigma(\gamma\pi \rightarrow \pi\pi)$
	 	$\Gamma_{3\pi}$	$\Gamma_{\pi^0\gamma}$ $\frac{d^2\Gamma}{dsdr}(\omega, \phi \rightarrow 3\pi)$
	 	$F_{3\pi}$	$\sigma(e^+e^- \rightarrow \pi^0\gamma)$ $\sigma(e^+e^- \rightarrow 3\pi)$ $\sigma(\gamma\pi \rightarrow \pi\pi)$ $\frac{d^2\Gamma}{dsdr}(\omega, \phi \rightarrow 3\pi)$ $\sigma(e^+e^- \rightarrow 3\pi)$

Table 1: Processes and unitarity relations relevant for the pion transition form factor. The three panels represent $q_s^2 = 0$, $q_s^2 = M_\omega^2, M_\phi^2$, and general q_s^2 . The last two columns refer to observables necessary to fix indispensable (SC 1) and optional (SC 2) subtractions, respectively. $\gamma_{v/s}$ denotes isovector/isoscalar photons, capital letters the partial wave relevant for the $\pi\pi$ rescattering. The last line is not formally a unitarity relation, but describes the parametrization of $\sigma(e^+e^- \rightarrow 3\pi)$.

process	building blocks and SC
	$\alpha_1 \pm \beta_1, \alpha_2 \pm \beta_2$ $\alpha_1(q^2) \pm \beta_1(q^2), \text{ChPT}$ $e^+e^- \rightarrow \pi\pi\gamma$ $e^+e^- \rightarrow e^+e^-\pi\pi$ ChPT $(e^+e^- \rightarrow \pi\pi\gamma)$ $e^+e^- \rightarrow e^+e^-\pi\pi$

Table 2: Processes and unitarity relations relevant for the $\gamma^*\gamma^* \rightarrow \pi\pi$ partial waves. The last column refers to data that are required to determine subamplitudes and fix subtraction constants (SC). Processes in the upper panel are needed for the reconstruction of the left-hand cut, while the diagrams in the lower panel represent the right-hand cut in real, singly-virtual, and doubly-virtual $\gamma\gamma$ fusion. In the doubly-virtual case, $e^+e^- \rightarrow \pi\pi\gamma$ is put in brackets since not all subtraction constants can be determined from singly-virtual data alone.

$e^+e^- \rightarrow e^+e^-\pi\pi$. For the singly-virtual case in the space-like region the subtraction function can be expressed in terms of generalized pion polarizabilities $\alpha_1(q^2) \pm \beta_1(q^2)$. Moreover, the doubly-virtual subtraction functions are already partially constrained by singly-virtual input, so that in combination with ChPT a first estimate should be possible even absent doubly-virtual data. These aspects are represented by the lower panel of Table 2.

4. Higher intermediate states

Pseudoscalar poles with higher mass, most prominently η and η' , can be treated in the same way as sketched here for the pion pole, for first steps in this direction see [37, 38]. As alluded to in Sect. 2.2, in the end the result of the dispersive calculation, valid in the low- and intermediate-energy region, has to be brought into accord with constraints from perturbative QCD, which can be interpreted as being generated by the exchange of even heavier pseudoscalar resonances [19].

As far as two-particle intermediate states are concerned, the discussion here generalizes immediately to $K\bar{K}$. In fact, in order to reproduce the dynamics in the isospin-zero S -wave in the region of the $f_0(980)$ correctly, even a coupled-channel treatment of the $\pi\pi/K\bar{K}$ system for this partial wave will become necessary. Further intermediate states, e.g. with more than two pions, are more difficult to account for at the same level of rigor as presented here. Possible approaches would be to estimate effects of missing degrees of freedom in terms of an effective resonance description [39], to cluster particles into effective two-particle intermediate states for which a variant of (2) should exist, or to try to find a generalization of the FsQED calculation including resonances, all of which concern possible future extensions of the formalism. The most important effective-resonance contributions not coupling to $\pi\pi$ appear to be axial vectors $a_1(1260)$ and $f_1(1285)$, as well as the scalar and tensor states of isospin $I = 1$, coupling to the $\pi\eta/K\bar{K}$ system, the $a_0(980)$ and $a_2(1320)$. Sum-rule constraints relating different such resonance contributions [40] should be taken into account where possible. Apart from such estimates, clearly more work is needed to incorporate constraints from perturbative QCD.

5. Relation to previously considered contributions

We wish to briefly comment on the relation of the dispersive analyses of π^0 -pole and $\pi\pi$ -cut contributions to the HLbL tensor in the context of previous analyses.

The pseudoscalar pole terms with their associated form factors are mostly analyzed within vector-meson-dominance (VMD) models and extensions thereof [12, 15, 17, 19, 21, 41]. However, arguably the only experimental information we have on the doubly-virtual π^0 transition form factor, via the conversion decay $\omega \rightarrow \pi^0\mu^+\mu^-$, seems to indicate very dramatic deviations from a simple VMD picture [42, 43]. While there are doubts about the consistency of these form factor data with what is obtained, in a different kinematic regime, from $e^+e^- \rightarrow \omega\pi^0$ [44–47], enhancements in the (isovector) slope by more than 40% are also found in a theoretical dispersive description [26].

The dispersive approach to include two-pion-cut contributions to the HLbL tensor comprises various effects that have been discussed separately in the literature. It is the only sensible way to include the $f_0(500)$ scalar meson, with its pole position deep inside the complex plane [48], and—once generalized to a two-channel analysis including $K\bar{K}$ —certainly the cleanest for the $f_0(980)$, too. Even the largest tensor-meson effect, through the $f_2(1270)$ [39], is covered by the $\pi\pi$ D -wave contribution,

as the $f_2(1270)$ is still dominantly elastic. Furthermore, the effects of pion polarizabilities on HLbL [49, 50] are automatically taken into account.

6. Conclusions

In this letter we have given an overview of recent theoretical developments that will pave the way for a data-driven approach also to the calculation of the HLbL contribution to a_μ . We have offered a detailed account of which processes can help constrain the contribution from one- and two-pion intermediate states to HLbL scattering. In particular, we have discussed how information from other processes can provide a handle on the dependence on the photon virtualities even in the absence of doubly-virtual measurements, and specified the unitarity relations that are instrumental in establishing this bridge. We are confident that with the methods outlined here a more data-driven and thus less model-dependent evaluation of the HLbL contribution to the muon $g - 2$ is feasible.

Acknowledgements

We would like to thank David W. Hertzog and Martin J. Savage for discussions that prompted the preparation of this letter, as well as Simon Eidelman and Andrzej Kupść for comments on the manuscript. Financial support by the Swiss National Science Foundation, the DFG (CRC 16, “Subnuclear Structure of Matter”), and by the project “Study of Strongly Interacting Matter” (HadronPhysics3, Grant Agreement No. 283286) under the 7th Framework Program of the EU is gratefully acknowledged.

References

[1] F. Jegerlehner and A. Nyffeler, Phys. Rept. **477** (2009) 1 [arXiv:0902.3360 [hep-ph]].
 [2] J. Prades, E. de Rafael and A. Vainshtein, Advanced series on directions in high energy physics 20 [arXiv:0901.0306 [hep-ph]].
 [3] T. Blum *et al.*, arXiv:1311.2198 [hep-ph].
 [4] M. Benayoun *et al.*, arXiv:1407.4021 [hep-ph].
 [5] J. Calmet, S. Narison, M. Perrottet and E. de Rafael, Phys. Lett. B **61** (1976) 283.
 [6] A. Kurz, T. Liu, P. Marquard and M. Steinhauser, Phys. Lett. B **734** (2014) 144 [arXiv:1403.6400 [hep-ph]].
 [7] G. Colangelo, M. Hoferichter, A. Nyffeler, M. Passera and P. Stoffer, Phys. Lett. B **735** (2014) 90 [arXiv:1403.7512 [hep-ph]].
 [8] G. Colangelo, M. Hoferichter, M. Procura and P. Stoffer, arXiv:1402.7081 [hep-ph].
 [9] E. de Rafael, Phys. Lett. B **322** (1994) 239 [hep-ph/9311316].
 [10] J. Bijnens, E. Pallante and J. Prades, Phys. Rev. Lett. **75** (1995) 1447 [Erratum-ibid. **75** (1995) 3781] [hep-ph/9505251].
 [11] J. Bijnens, E. Pallante and J. Prades, Nucl. Phys. B **474** (1996) 379 [hep-ph/9511388].
 [12] J. Bijnens, E. Pallante and J. Prades, Nucl. Phys. B **626** (2002) 410 [hep-ph/0112255].
 [13] M. Hayakawa, T. Kinoshita and A. I. Sanda, Phys. Rev. Lett. **75** (1995) 790 [hep-ph/9503463].
 [14] M. Hayakawa, T. Kinoshita and A. I. Sanda, Phys. Rev. D **54** (1996) 3137 [hep-ph/9601310].
 [15] M. Hayakawa and T. Kinoshita, Phys. Rev. D **57** (1998) 465 [Erratum-ibid. D **66** (2002) 019902] [hep-ph/9708227 [hep-ph/0112102]].

[16] M. Knecht, A. Nyffeler, M. Perrottet and E. de Rafael, Phys. Rev. Lett. **88** (2002) 071802 [hep-ph/0111059].
 [17] M. Knecht and A. Nyffeler, Phys. Rev. D **65** (2002) 073034 [hep-ph/0111058].
 [18] M. J. Ramsey-Musolf and M. B. Wise, Phys. Rev. Lett. **89** (2002) 041601 [hep-ph/0201297].
 [19] K. Melnikov and A. Vainshtein, Phys. Rev. D **70** (2004) 113006 [hep-ph/0312226].
 [20] T. Goecke, C. S. Fischer and R. Williams, Phys. Rev. D **83** (2011) 094006 [Erratum-ibid. D **86** (2012) 099901] [arXiv:1012.3886 [hep-ph]].
 [21] P. Roig, A. Guevara and G. L. Castro, Phys. Rev. D **89** (2014) 073016 [arXiv:1401.4099 [hep-ph]].
 [22] T. Blum, M. Hayakawa and T. Izubuchi, arXiv:1407.2923 [hep-lat].
 [23] E. Czerwiński *et al.*, arXiv:1207.6556 [hep-ph].
 [24] F. Niecknig, B. Kubis and S. P. Schneider, Eur. Phys. J. C **72** (2012) 2014 [arXiv:1203.2501 [hep-ph]].
 [25] M. Hoferichter, B. Kubis and D. Sakkas, Phys. Rev. D **86** (2012) 116009 [arXiv:1210.6793 [hep-ph]].
 [26] S. P. Schneider, B. Kubis and F. Niecknig, Phys. Rev. D **86** (2012) 054013 [arXiv:1206.3098 [hep-ph]].
 [27] M. J. Amarian *et al.*, arXiv:1308.2575 [hep-ph].
 [28] R. García-Martín and B. Moussallam, Eur. Phys. J. C **70** (2010) 155 [arXiv:1006.5373 [hep-ph]].
 [29] M. Hoferichter, D. R. Phillips and C. Schat, Eur. Phys. J. C **71** (2011) 1743 [arXiv:1106.4147 [hep-ph]].
 [30] B. Moussallam, Eur. Phys. J. C **73** (2013) 2539 [arXiv:1305.3143 [hep-ph]].
 [31] M. Hoferichter, G. Colangelo, M. Procura and P. Stoffer, arXiv:1309.6877 [hep-ph].
 [32] S. Mandelstam, Phys. Rev. Lett. **4** (1960) 84.
 [33] W. Lucha, D. Melikhov and S. Simula, Phys. Rev. D **75** (2007) 016001 [hep-ph/0610330].
 [34] K. M. Watson, Phys. Rev. **95** (1954) 228.
 [35] M. Hoferichter, B. Kubis, S. Leupold, F. Niecknig and S. P. Schneider, in preparation.
 [36] A. Aloisio *et al.* [KLOE Collaboration], Phys. Lett. B **561** (2003) 55 [Erratum-ibid. B **609** (2005) 449] [hep-ex/0303016].
 [37] C. Hanhart, A. Kupść, U.-G. Meißner, F. Stollenwerk and A. Wirzba, Eur. Phys. J. C **73** (2013) 2668 [arXiv:1307.5654 [hep-ph]].
 [38] F. Stollenwerk, C. Hanhart, A. Kupść, U.-G. Meißner and A. Wirzba, Phys. Lett. B **707** (2012) 184 [arXiv:1108.2419 [nucl-th]].
 [39] V. Pauk and M. Vanderhaeghen, arXiv:1401.0832 [hep-ph].
 [40] V. Pascalutsa, V. Pauk and M. Vanderhaeghen, Phys. Rev. D **85** (2012) 116001 [arXiv:1204.0740 [hep-ph]].
 [41] P. Masjuan, Phys. Rev. D **86** (2012) 094021 [arXiv:1206.2549 [hep-ph]].
 [42] R. Arnaldi *et al.* [NA60 Collaboration], Phys. Lett. B **677** (2009) 260 [arXiv:0902.2547 [hep-ph]].
 [43] G. Usai [NA60 Collaboration], Nucl. Phys. A **855** (2011) 189.
 [44] M. N. Achasov *et al.* [SND Collaboration], Phys. Lett. B **486** (2000) 29 [hep-ex/0005032].
 [45] R. R. Akhmetshin *et al.* [CMD-2 Collaboration], Phys. Lett. B **562** (2003) 173 [hep-ex/0304009].
 [46] F. Ambrosino *et al.* [KLOE Collaboration], Phys. Lett. B **669** (2008) 223 [arXiv:0807.4909 [hep-ex]].
 [47] M. N. Achasov *et al.* [SND Collaboration], Phys. Rev. D **88** (2013) 5, 054013 [arXiv:1303.5198 [hep-ex]].
 [48] I. Caprini, G. Colangelo and H. Leutwyler, Phys. Rev. Lett. **96** (2006) 132001 [hep-ph/0512364].
 [49] K. T. Engel, H. H. Patel and M. J. Ramsey-Musolf, Phys. Rev. D **86** (2012) 037502 [arXiv:1201.0809 [hep-ph]].
 [50] K. T. Engel and M. J. Ramsey-Musolf, arXiv:1309.2225 [hep-ph].